Pharmaceutical Research, Vol. 26, No. 11, November 2009 (© 2009)
DOI: 10.1007/s11095-009-9963-6

Research Paper

Carboxylate-Dependent Gelation of a Monoclonal Antibody

Osigwe Esue,[1,3] Sonoko Kanai,[2] Jun Liu,[2] Thomas W. Patapoff,[1] and Steven J. Shire[2]

Received May 3, 2009; accepted August 20, 2009; published online September 3, 2009

Purpose. This paper shows the first ever assembly of monoclonal antibody using multivalent carboxylate ions into highly ordered structures that feature viscoelastic properties reminiscent of other filamentous proteins.
Methods. A monoclonal antibody was assembled into filamentous networks by adding multivalent carboxylates to the protein solution. Gelation and characterization of these networks were monitored using mechanical rheometry, electron microscopy, Fourier transform infra-red and Raman spectroscopy.
Results. Electron microscopy and mechanical rheometry suggest the formation of rigid filament bundles that feature strong interfilament interactions. Filament network elasticity increased with multivalent carboxylate and protein concentrations, hinting at the importance of multivalent carboxylates in the mechanism of assembly.
Conclusion. Assembly is not triggered by high ionic strength but with multivalent carboxylates. A high protein concentration is required for filament formation and the elasticity of the networks are weakly dependent on concentration. The exact mechanism of assembly is still elusive, although we speculate that carboxylates could act as a bridge to crosslink antibody monomers. These monoclonal antibody monomers could be linked either through Fab-Fab or Fc-Fab regions, although previous reports have shown evidence of reversible self-association mediated through the Fab regions.

KEY WORDS: carboxylates; cryoglobulins; gelation; mechanical properties; monoclonal antibody; self-association; structure; viscosity.

INTRODUCTION

Monoclonal antibodies function to identify antigens in the body; this unique ability makes their use as therapeutics increasingly widespread (1–3). Either marketed or in clinical development, they are used in treating various indications in areas such as oncology, immunology, and cardiovascular repair (4–7). There are different antibody isotypes existing as either soluble secreted proteins in the body or as B-cell bound receptors. Some of these isotypes form multimers that bind to foreign epitopes with increased avidity to form larger complexes (8) and may enhance antibody-dependent cell cytotoxicity processes (9–12).

Previous studies suggest that, reversibly, self-association of antibodies can be enhanced at high concentrations (13–16), and they can naturally assemble into polymers (cryoglobulins) at reduced temperatures (<5°C) (16–19). Although specific antibodies may not be present at such high concentrations *in vivo*, during infections, B-cells secrete increased amounts of antibodies into an already molecularly crowded environment. A molecularly crowded environment presents deviations from ideality, resulting in more complicated interactions, whereby interactions between protein molecules and their solution excipients may become more prevalent (20,21). Understanding these interactions is challenging due to limited analytical methods. Recent findings using small angle x-ray and neutron scattering suggest the increases of attractive or repulsive interactions at high protein concentrations (22,23).

Poskitt *et al*. suggested that polymerized antibodies could activate the complement system through an alternate C3 proactivator (24). If these structures are present *in vivo*, they may increase binding avidity to receptors, which could increase efficiency of the C1q complement system or improve antibody-dependent cell cytotoxicity through NK cells. These suggest a possibly unexplored scope of structure-function relationship of antibodies. Consequences could include irreversible or reversible aggregation resulting in increased opalescence, turbidity, viscosity or precipitation (15,25); hence, understanding the conditions that trigger structured/unstructured aggregation of antibodies is important in development of stable and robust protein formulations for drug delivery. Alternatively, a controlled generation of stable and larger structures may allow for the generation of suspensions at high concentration with acceptable viscosity properties for delivery by the subcutaneous route (26).

[1] Early Stage Pharmaceutical and Device Development, Genentech Inc., 1 DNA Way, South San Francisco, California 94080, USA.
[2] Late Stage Pharmaceutical Development, Genentech Inc., 1 DNA Way, South San Francisco, California 94080, USA.
[3] To whom correspondence should be addressed. (e-mail: esue.osigwe@gene.com)

ABBREVIATION: MAb, monoclonal antibody.

Using electron microscopy, time-resolved rheometry, Fourier-transform infra-red and Raman spectroscopy, we investigated the assembly and structure of a monoclonal antibody in the presence of carboxylate-containing buffers. We find that the monoclonal antibody assembles in the presence of multivalent carboxylate ions, not monovalent, unlike some cryoglobulins that were found to assemble in the presence of some divalent metal ions—calcium, barium, manganese and strontium (27).

MATERIALS AND METHODS

Sample Preparation

A humanized monoclonal antibody, MAb, was constructed from an IgG1 human framework with κ light chains. This antibody was expressed in Chinese hamster ovary (CHO) cell lines and isolated by a series of chromatography methods including protein A affinity chromatography and ion exchange chromatography. Buffers during purification and final formulation steps were exchanged using Tangential Flow Filtration (TFF) processes. The antibody (MW= 150 KDa; pI=7.5), which is stored in 30 mM histidine hydrochloride buffer at pH 6.0, has a theoretical pI and net charge of 7.5 and 17.7, respectively. The theoretical net charge, measured by amino acid composition, could be substantially different from the measured net charge as determined by membrane-confined electrophoresis (28,29). All the chemical reagents were analytical grade or higher.

Concentration Determination

The concentration of antibody was obtained using a Hewlett Packard 8453 diode array spectrophotometer with a 1-cm quartz cuvette. The concentration was calculated using an absorptivity of 1.60 cm^{-1} $(mg/ml)^{-1}$ for MAb as determined by quantitative amino acid analysis.

Quantitative Rheology Measurement

The visco-elastic properties of MAb solution were measured at 25°C with a temperature-controlled cone and plate MCR300 rheometer (Anton Paar, Ashland, VA) equipped with a solvent trap to prevent solvent evaporation. The reported value is an average of two runs. Assembly of MAb into filamentous structures was initiated by addition of millimolar concentrations of sodium citrate. The cone is attached to a motor which applies an oscillatory shear deformation with controlled frequency and amplitude. A torque transducer which attaches to the cone measures the stress induced by the shear deformation within the MAb solution. The instrument calculates the elastic (storage) modulus, G′, and the viscous (loss) modulus, G″, respectively. The kinetics and extent of gelation of MAb solutions were monitored by measuring the elastic and viscous moduli, G′ and G″, at 1 rad/s and 0.1% strain every 30 s for 10 h unless otherwise specified. At a steady state, the frequency-dependent elastic and viscous moduli, G′(ω) and G″(ω), were measured by applying 0.1% amplitude oscillatory deformations of frequencies between 0.01 and 100 rad/s.

Electron Microscopy (EM)

The structure of MAb solutions were probed using electron microscopy. 10 μl of assembled MAb solutions was placed on an electron microscope grid. The grids were washed and stained with 2% uranyl acetate solution (30). The excess stain was drained off at a 45° angle on a filter paper and dried. Electron microscopy was performed using a Phillips 410 transmission electron microscope with a magnification between 50,000× and 105,000×.

Raman Spectroscopy

All spectra were collected from 1,772–710 cm^{-1} using a Nicolet Almega XR Dispersive Raman Spectrometer (Thermo Fisher Scientific, Waltham, MA). The laser wavelength employed was 532 nm, and each recorded spectrum was a result of 5 exposures with 10 s of accumulation per exposure.

Fourier Transform Infra-Red Spectroscopy (FTIR)

FT-IR measurements were measured at room temperature on a Nicolet FT-IR spectrometer equipped with a zinc selenide attenuated total reflection (ATR) accessory. The method used a resolution of 4 cm and an average of 256 scans per spectra. A spectrum of a 150 mg/ml antibody solution was taken before and after assembly caused by addition of carboxylate buffers. The spectra were corrected by subtracting spectra of corresponding buffers of both assembled and unassembled proteins using 2,200 cm^{-1} and 1,800 cm^{-1} region that had no characteristic peaks.

RESULTS

Monoclonal Antibodies Can Form Viscoelastic Gels

Antibodies isolated from patients with specific disease states assemble into filamentous structures at reduced temperatures; however, the assembly of these structures is not well-controlled and understood (16,24,27). We found that under certain conditions, we can reproducibly and in a controlled fashion assemble a MAb into well-ordered filamentous structures that feature viscoelastic properties reminiscent of other viscoelastic protein assemblies (30–32). We monitored the time-dependent gelation of a 125 mg/ml MAb solution by using a cone-and-plate rheometer to monitor the network's elasticity (*i.e.* stiffness) at a fixed frequency and deformation amplitude. Gelation is defined here as the process of formation of a stiff network presumably caused by the onset of topological overlaps among polymerizing MAb or filaments as well as the cross-linking and bundling of these filaments. This stiff network manifests as a solution elastic modulus (G′) as well as an increase in its inherent viscous modulus (G″) (33,34). The cone-and-plate rheometer measures and reports an elastic modulus, G′ (the propensity of the polymers to rebound after shear deformation), a viscous modulus, G″ (the flow or resistance to flow of a sample after shear deformation), and a phase angle, which compares the elastic and viscous nature of a material. This phase angle, = $\tan^{-1}(G''/G')$, is directly obtained from values of G′ and G″. An elastic solid, like rubber, exhibits a phase

angle of 0° (G′>>G″), while a purely viscous liquid, such as water or glycerol, exhibits a phase angle of 90° (G″>>G′). Viscoelastic solutions feature a phase angle, 0° << 90° (33,34). The kinetics and extent of gelation of MAb solutions were monitored by measuring the elastic and viscous moduli, G′ and G″, at 1 rad/s and 0.1% strain unless otherwise stated. A strain amplitude of 0.1% was determined to be non-destructive to the filament networks and hence within its linear stress regime (not shown).

Gelation of MAb was triggered by the addition of millimolar concentrations of sodium citrate (Fig. 1). Solutions of unassembled MAb solutions (125 mg/ml) showed no elastic modulus (Fig. 1A, *inset*). Upon addition of 5 mM citrate, the elastic modulus of MAb solutions increased after a long lag phase (Fig. 1A, *inset*). This lag phase decreased with increase in citrate concentration and was completely eliminated in the presence of 100 mM citrate. After 10 h of gelation, the elastic modulus, G′, of 125 mg/ml MAb ranged from 2,000 Pa to 10,000 Pa with 10 mM and 100 mM citrate, respectively (Fig. 1A, B).

MAb solutions with ≤5 mM citrate formed gels that were more viscous than elastic, a solution property that was quickly reversed above 10 mM citrate (Fig. 1B). At citrate concentrations above 10 mM citrate, MAb solutions gradually became more solid-like with time, as seen by its quickly reducing phase angle (Fig. 1C). Solutions containing 100 mM citrate were most solid-like, featuring a phase angle of 18° after 10 h (Fig. 1C, *inset*). After gelation, the tendency of MAb filaments to move in solution was tested by subjecting the solution to a constant shear deformation of increasing frequency (Fig. 1D). In the presence of 5 mM citrate, the elastic modulus of MAb solution increased ~25-fold from 20 Pa to 500 Pa with increasing frequency, from 0.01 rad/s to 100 rad/s, respectively, consistent with untangled or loosely entangled filaments in solution. Highly entangled filament networks, on the other hand, are less dependent on the frequency as observed with higher concentrations of citrate (100 mM) where the elastic modulus only increases by 6-fold over the same frequency range tested (Fig. 1D). This suggests that MAb filaments are less flexible in the presence of higher concentrations of citrate, presumably due to increased interfilament interactions.

Citrate Mediates the Formation of Stiff and Rigid MAb Filaments

Results obtained from rheological measurements were complemented with electron micrographs (Figs. 2 and 3F). We conducted negative staining and electron microscopy to investigate the morphology of filaments of 50 mg/ml MAb assembled in 50 mM citrate. MAb formed straight filament bundles that appeared rigid (Fig. 2). Analysis of micrographs showed big bundles containing smaller filament bundles. These big bundles varied widely in length up to 3 μm and had diameters as large as 200 nm, while the smaller bundles ranged in diameter from 29 nm to 55 nm (Fig. 2). The smaller bundles were made up of straight single filaments with an average diameter of 4 nm in agreement with the hydrodynamic size of unassembled MAb monomers measured by dynamic light scattering (not shown). FTIR and Raman spectroscopy, which are sensitive to the secondary structure of proteins (35,36), suggested that the assembly of MAb does not feature a significant change in secondary structure before and after the addition of citrate (not shown).

Mechanical Properties of Monoclonal Antibody Networks Are Concentration-Dependent

To fully characterize the mechanical properties of MAb, we measured the extent and rate of gelation of MAb over a wide range of concentrations. The elastic modulus of MAb at 50 mM citrate increases with MAb concentration (Fig. 3A). The rate of gelation as monitored by the increase in elastic modulus was much faster during the first hour. This is consistent with growth and overlap of polymerizing filaments, after which the filaments form a more homogeneous network with time (2–10 h) (37). Assembled 25 mg/ml MAb solution displayed little elastic modulus (10^{-8} Pa), while at ≥100 mg/ml, there is a steep increase in the elastic modulus of MAb solutions; the elastic modulus at 50 mg/ml and 125 mg/ml is 0.1 Pa and 3,000 Pa, respectively (Fig. 3A, *inset*). Since EM shows evidence of filamentous structures at 50 mg/ml, rheological results suggest that 50 mg/ml is less than its critical overlap concentration, C* (concentration at which the filaments in solution grow long enough and begin to overlap to form an extensive network and, ultimately, an increased modulus). While the lag phase reduced with concentration, the rate of assembly of MAb networks, measured by the time to reach 90% of its steady-state elastic modulus, increased steadily with MAb concentration (Fig. 3B), consistent with the presence of increased density and thickness of filament bundles resulting in longer times for the network to become more homogeneous. The higher the concentration of MAb, the stiffer the networks they form (Fig. 3C). The phase angle for 25 mg/ml solutions was ~90°, indicative of a viscous solution, while at concentrations ≥50 mg/ml solution, the phase angle reduced significantly to ~20°–30° resulting in a more solid-like network at steady state (Fig. 3C).

After 10 h of gelation, elastic and viscous moduli were measured as a function of frequency to probe network dynamics (Fig. 3D, E). The elastic modulus of MAb networks increased with increasing shear frequency. This test describes the ability of filaments to move in solution to relax the induced mechanical stress (Fig. 3D). The profiles of elastic modulus as a function of frequency, ω, can be fit with a power law $G'(\omega) \sim \omega^a$, with an exponent, *a,* that describes the steepness of the frequency dependence of $G'(\omega)$. For a frequency region of 1 to 100 rad/s, the exponent, *a,* remained relatively constant at a fixed citrate concentration of 50 mM with increasing MAb concentration from 50 mg/mL to 125 mg/mL (except 25 mg/ml, which had very low elasticity) (Fig. 3E). On the other hand the exponent slightly decreased with increasing citrate concentration for a fixed MAb concentration at 125 mg/mL (Fig. 3E *inset*), which suggests less relative movements among filaments under these conditions (or enhanced interaction between filaments). Filaments in a network of fixed polymer length and concentration interact through their cross-linking interactions, hence affecting their mobility.

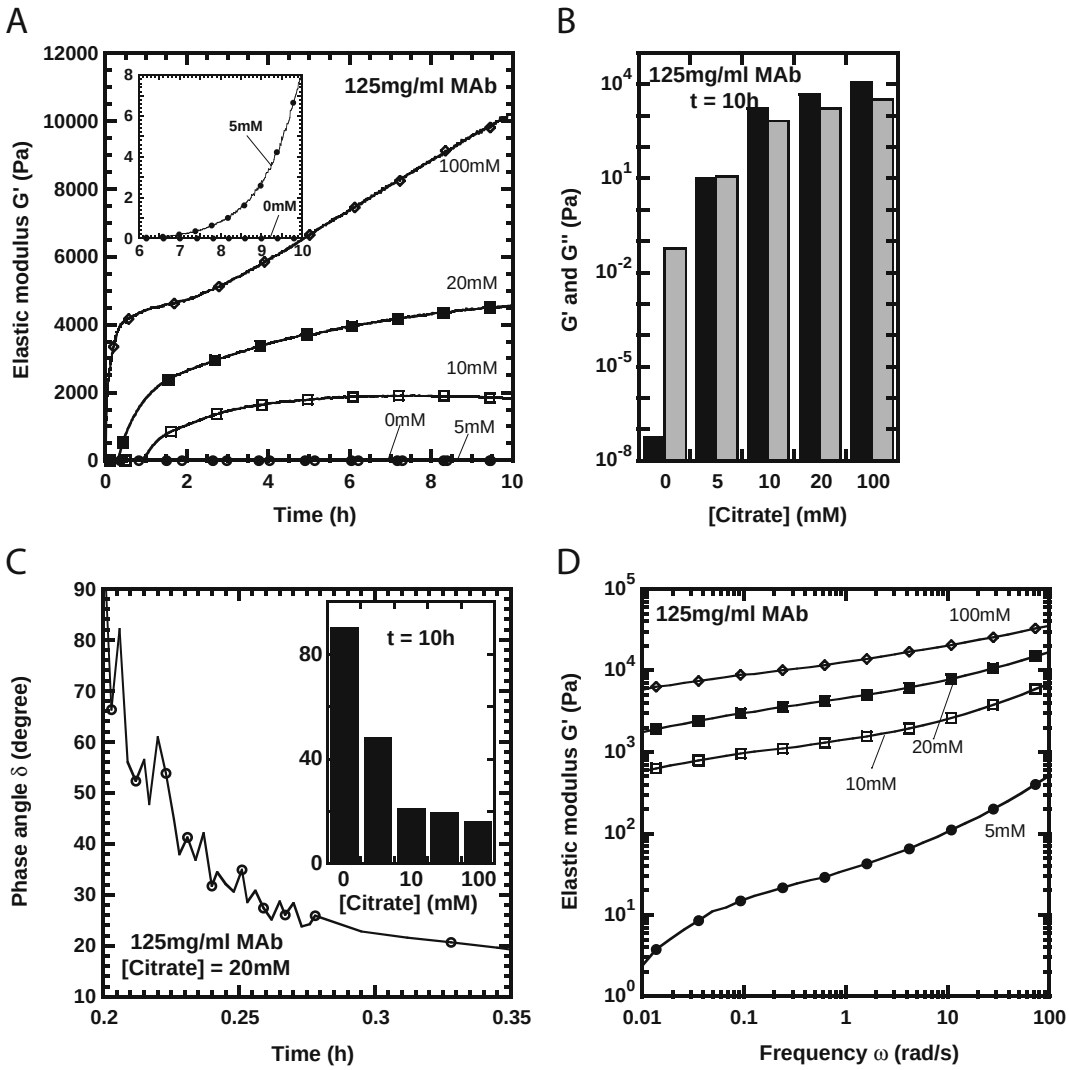

Fig. 1. Gelation of MAb. **A** Increase in elasticity, G′, of 125 mg/ml MAb solution upon addition of citrate. *Inset*, elasticity of 125 mg/ml MAb with 5 mM citrate showing prolonged lag phase. Sodium citrate concentrations are 0 mM (*open circles*), 5 mM (*closed circles*), 10 mM (*open squares*), 20 mM (*closed squares*), and 100 mM (*open diamonds*). **B** Profile showing the elasticity, G′, (*black bars*) and viscous modulus, G′′, (*grey bars*) of MAb gels after 10 h of gelation as a function of citrate concentration. **C** Phase angle (*open circles*) of MAb gels in 20 mM citrate over time. The phase angle describes the delay between imposed deformation and resulting stress in the gels. The phase angle is 90° for a viscous liquid like water or glycerol, which has no elasticity, and 0° for a highly elastic material like a crosslinked polyacrylamide gel. *Inset*, Profile showing the phase angle of MAb gels after 10 h of gelation as a function of citrate concentration. **D** Frequency-dependent elasticity, G′(ω), of 125 mg/ml MAb solutions for varying citrate concentrations. Sodium citrate concentrations are 0 mM (*open circles*), 5 mM (*closed circles*), 10 mM (*open squares*), 20 mM (*closed squares*), and 100 mM (*open diamonds*). The amplitude of shear deformations and frequency in all experiments was 0.1% and 1 rad/s, respectively, unless otherwise stated.

Multivalent Carboxylate Ions Assemble MAb

We hypothesized that MAb monomers could be assembled in other carboxylates, such as acetate (mono-carboxylate) and succinate (di-carboxylate). Gelation was monitored by the increase in elastic modulus after adding 100 mM carboxylates at pH 6 to MAb solutions at 125 mg/mL. In the presence of the monovalent ion, acetate, there was no increase in elastic modulus even after 14 h (Fig. 4A). However, addition of a divalent ion, succinate, to MAb solution resulted in an increase in its solution elastic modulus with a long lag phase (~4 h) (Fig. 4A). Over time, solutions containing acetate consistently exhibited liquid-like character as indicated by a phase angle of ~90°, while succinate-containing solutions gradually became more solid-like with time. Addition of citrate, on the other hand, instantly generated MAb solutions with more solid-like properties (Fig. 4B). Since acetate, succinate, and citrate all have different pKas', there would be a different distribution of carboxylate ions in solution at pH 6.0. To ascertain the impact of ionic strength, we added 300 mM acetate to a 125 mg/ml MAb solution (Fig. 5). The high ionic strength solution of MAb still exhibited negligible elasticity, suggesting that the assembly of MAb is not triggered by high ionic strength but requires the presence of multivalent carboxylates such as succinate and citrate.

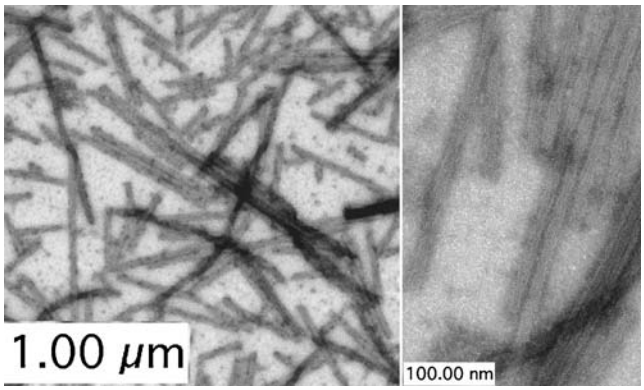

Fig. 2. Structure of MAb filaments. Electron micrographs of 50 mg/ml MAb after the addition of sodium citrate. Analysis of micrographs showed big bundles containing smaller filament bundles. Individual straight filaments were of varying lengths and had an average diameter of 4 nm. Scale bars are 1 μm and 100 nm.

DISCUSSION

Antibodies function to direct immune responses in living organisms. *In vivo*, they can form smaller structures from dimers to pentamers, enabling them to bind foreign epitopes with increased avidity and forming larger complexes (8), while *in vitro*, they can self-associate reversibly at high concentrations (14). In certain disease states, immunoglobulins form insoluble aggregates *in vivo* (17,38). These insoluble aggregates have not been isolated intact and analyzed; however, immunoglobulins have been purified from the plasma of infected patients, and aggregates triggered by lowering solution temperature (16,24). Here we report a novel characteristic of a monoclonal antibody, in the presence of multivalent carboxylates, to reproducibly assemble into filaments that overlap to form well-organized structures and

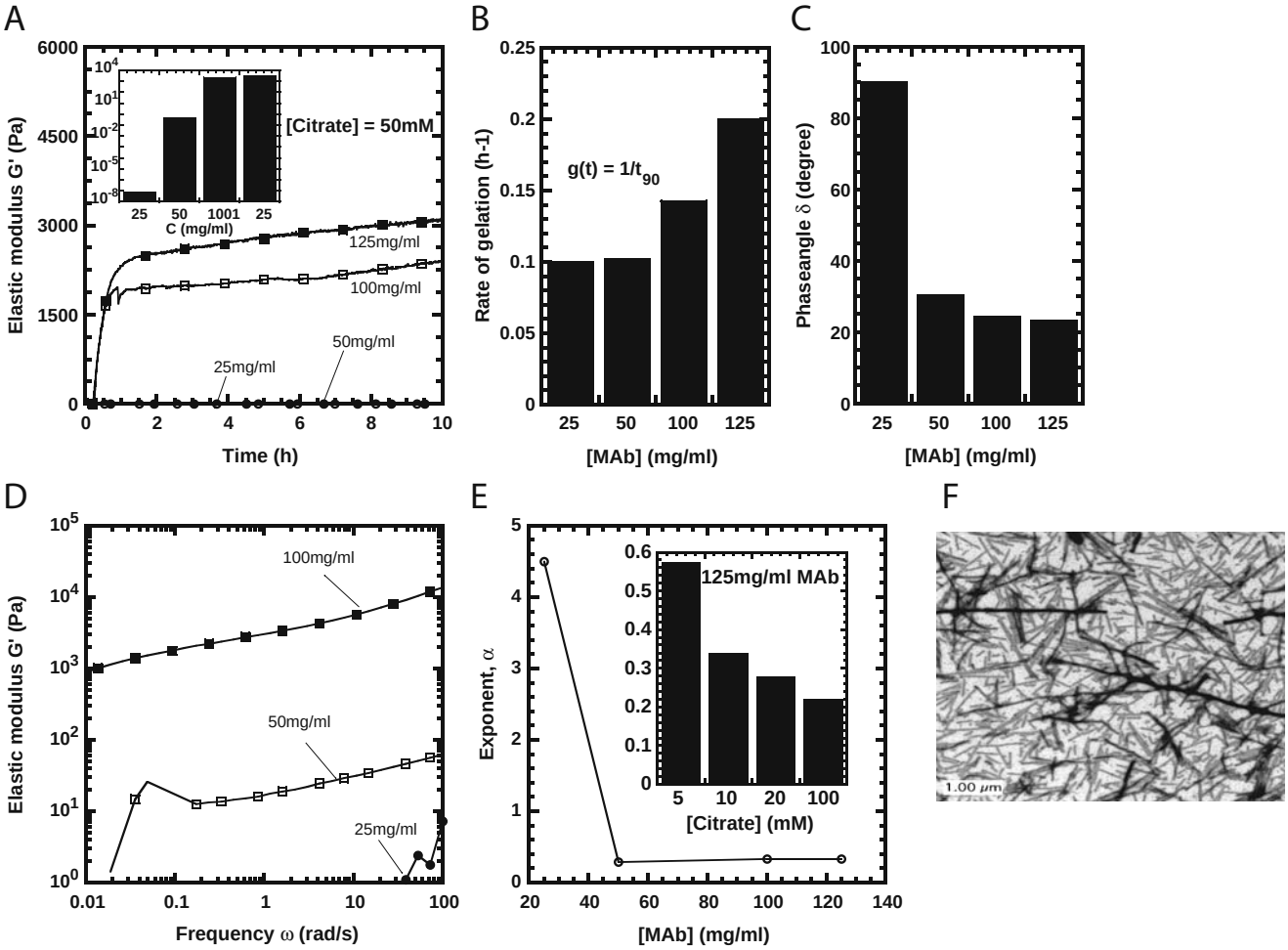

Fig. 3. Elasticity of MAb gels is concentration-dependent. **A** Increase in elasticity, G′, of MAb solution upon addition of 50 mM citrate. MAb concentrations are 25 mg/ml (*open circles*), 50 mg/ml (*closed circles*), 100 mg/ml (*open squares*), and 125 mg/ml (*closed squares*). *Inset*, Steady-state elasticity of MAb after 10 h of gelation. **B** Rate of gelation as a function of MAb concentration. The rate of gelation is defined as the inverse time required to get to 90% of the gel elasticity at 10 h. **C** Steady-state phase angle as a function of MAb concentration after 10 h of gelation. **D** Frequency-dependent elasticity, G′(ω), of 25 mg/ml (*closed circles*), 50 mg/ml (*open squares*), 100 mg/ml (*closed squares*) MAb gels. The frequency ω describes the rate at which the network is deformed by oscillatory shear deformations; frequencies were increased from low to high values. **E** Exponent, *a,* describes the frequency dependence of the network elasticity as a power law of the frequency ω, $G'(\omega) \sim \omega^a$, as a function of MAb concentration, assembled with 50 mM citrate. The exponent, a, decreases with concentration, implying that MAb gels contain filament that are less labile with MAb concentration. *Inset,* Exponent of 125 mg/ml gels decreases with increases in citrate concentration. The amplitude of shear deformations and frequency in all experiments was 0.1% and 1 rad/s, respectively, unless otherwise stated. **F** Analysis of micrographs showed big bundles within a filamentous network. Scale bar is 1 μm.

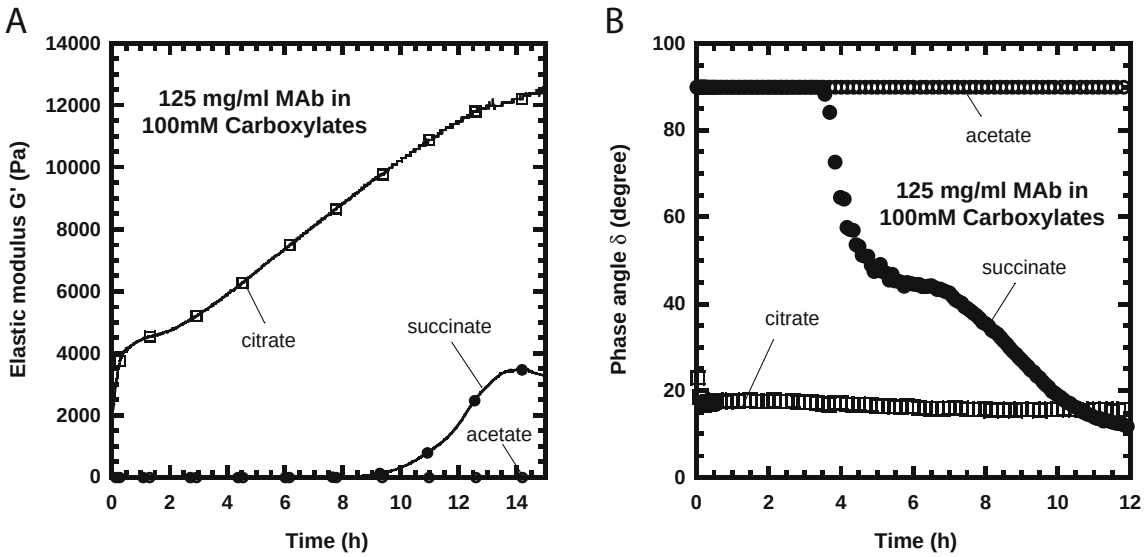

Fig. 4. Effect of multivalent carboxylate ions on MAb gelation. **A** Time-dependent elasticity and **B** Phase angle of a 125 mg/ml MAb solution with time upon addition of 100 mM carboxylates. Carboxylates used are citrate (*open squares*), succinate (*closed circles*), and acetate (*open circles*). The amplitude of shear deformations and frequency in all experiments was 0.1% and 1 rad/s, respectively.

feature mechanical properties that are reminiscent of other filamentous proteins (39). Previous studies suggest that antibodies can self-associate laterally through their Fab domain (13,16) and can assemble into polymers (cryoglobulins) at reduced temperatures (<5°C) (16–19). Our data suggests that antibodies may have a weak tendency to form filaments *in vitro*, since a very high concentration (~25 mg/ml) was required for gelation to occur. At such high concentrations, MAb gelation kinetics is slow, as it needs to overcome a threshold concentration required to form filaments that grow long enough to overlap into an elastic network. Although there is a relatively low tendency for assembly into filament bundles, these bundles are stable for days.

Naturally occurring biological structures that form bundles typically require auxiliary proteins that crosslink individual filaments into rigid structures similar to those formed by MAb (40). The elasticity of polymer networks are weakly dependent on either their intrinsic filament rigidity or their persistence length; hence, the high elastic modulus of MAb structures is mainly accounted for by strong interfilament interactions. These interfilament interactions are suggested by the presence of filament bundles observed by electron microscopy and the lack of strong shear frequency dependence by mechanical rheology. A high protein concentration (>25 mg/ml) was required for MAb to form polymers *in vitro*. Before the onset of an elastic modulus, the gels exhibit a long lag phase whereby filaments grow long enough to cause topological overlaps. The bundles, which are of varying length and thickness, imply some degree of a cooperative assembly mechanism. The mechanism of filament formation is still unclear. Do single filaments form that later bundle, or do bundles grow after the formation of a nucleus? We do not exclude the possibility of interaction through either lateral (Fab to Fab) or longitudinal (Fc to Fab) arrangements or both. The fact that assembly is dependent on the presence of carboxylates and that network elasticity is directly proportional to the carboxylates' concentration implies a more direct role of carboxylates in filament formation. Chaotropic anions have been shown to reduce the viscosity of proteins in a Hoffmeister series-dependent manner (13); citrate ions are one of the least chaotropic anions and, as such, may favor protein interactions. Polycarboxylates could act as a bridge between molecules, hence aiding the assembly of filaments and also crosslinking single filaments into bundles. Bundling is also possible through a counterion effect in which filament surface charges are neutralized, followed by filament-alignment by Van der Waal interactions (41), a phenomenon also described by the interaction potential and the Yukawa model of interacting proteins (42,43). The two-Yukawa potential has been used to predict the osmotic pressure of IgG proteins; however, this model is best used in solutions with low ionic strength and small self-association (44). On the other hand, in strongly associating systems, these parameters may not be

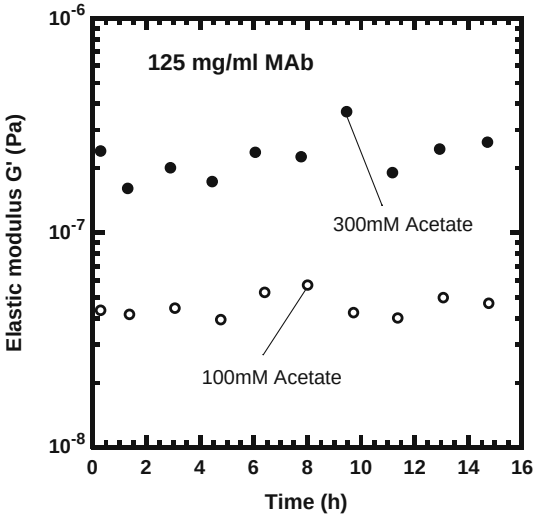

Fig. 5. Effect of ionic strength on MAb gelation. Elasticity of a 125 mg/ml MAb in 100 mM (*open circles*) and 300 mM sodium acetate (*closed circles*). The amplitude of shear deformations and frequency in all experiments was 0.1% and 1 rad/s, respectively.

predictive. A counterion effect, however, is less probable given the steep dependence of network elasticity on carboxylate ion concentration. Inter-protein interactions in these gels are significant since they interact to form filament bundles, and, hence, the classical equations for non-interacting systems such as the Mooney or Krieger-Dougherty equations are not applicable.

Network elasticity of the MAb tested is directly proportional to the concentration of multivalent carboxylates present in solution, implying that this carboxylate could act as a cross-linking agent. Above 25 mg/ml, the elasticity of these MAb gels is weakly dependent on increasing concentration, a feature that is consistent with rigid filaments (45–47). Another feature of rigid structures is exhibited by a low phase angle (47). MAb gels have a phase angle that decreases with increase in citrate or MAb concentration to a steady state of ~20°, which is comparable to other filamentous proteins, such as F-actin in the presence of cross-linking proteins, filamin. A phase angle of 90° implies the rheological behavior of a liquid, such as glycerol, whereas a phase angle close to 0° implies an elastic solid, such as a stiff rubber. This solid-like property can be further explained by stronger interfilament interactions suggested by probing MAb gels with varying shear rates. Rapidly applied deformations do not allow enough time for these polymers to relax, while slowly applied deformations allows polymers the time to rearrange and relax the stress. The elasticity at low concentrations of either MAb or carboxylate ion displays a frequency-dependent spectrum indicative of loosely overlapping or uncrosslinked filaments (48). In contrast, higher MAb concentrations feature frequency-independent elasticity, similar to cross-linked or bundled polymers. Our results imply that assembly and network rigidity are due to valence of carboxylates and not ionic strength. While increased ionic strength enhanced solution viscosity, it was not sufficient to form filaments.

In this report, we do not study the mechanism of assembly but convincingly show that a monoclonal antibody can form organized filamentous structures with strong interfilament interactions in the presence of multivalent carboxylates. We show the first evidence that monoclonal antibodies may indeed form larger structures and hypothesize that if this occurs *in vivo*, it may improve avidity of antibodies to their epitopes. The delivery of high-concentration antibodies has advantages for chronic indications, subcutaneous delivery, and reduced number of injections by minimizing injection volumes. However, the formation of large structures could also present safety concerns due to possible toxicities and immunogenicity. If these larger structures are therapeutically safe, they could be potentially beneficial in therapeutics.

ACKNOWLEDGEMENTS

We would like to thank Linda Rangell and Timothy Kamerzell for technical assistance with electron microscopy and technical discussions, respectively.

REFERENCES

1. Burrows W. The function of antibody in local immunity in the small bowel. Immunochemistry. 1975;12:621–3.
2. Peterson E, Owens SM, Henry RL. Monoclonal antibody form and function: manufacturing the right antibodies for treating drug abuse. AAPS J. 2006;8:E383–90.
3. Sutton BJ. Immunoglobulin structure and function: the interaction between antibody and antigen. Curr Opin Immunol. 1989;2:106–13.
4. Maggon K. Monoclonal antibody "gold rush". Curr Med Chem. 2007;14:1978–87.
5. Lao-araya M, Puthanakit T, Aurpibul L, Sirisanthana T, Sirisanthana V. Antibody response to hepatitis B re-vaccination in HIV-infected children with immune recovery on highly active antiretroviral therapy. Vaccine. 2007;25:5324–9.
6. Nabiand HA, Doerr RJ. Radiolabeled monoclonal antibody imaging (immunoscintigraphy) of colorectal cancers: current status and future perspectives. Am J Surg. 1992;163:448–56.
7. Wang J, Li H, Zou G, Wang LX. Novel template-assembled oligosaccharide clusters as epitope mimics for HIV-neutralizing antibody 2G12. Design, synthesis, and antibody binding study. Org Biomol Chem. 2007;5:1529–40.
8. Roux KH. Immunoglobulin structure and function as revealed by electron microscopy. Int Arch Allergy Immunol. 1999;120:85–99.
9. Natsume A, Wakitani M, Yamane-Ohnuki N, Shoji-Hosaka E, Niwa R, Uchida K, *et al*. Fucose removal from complex-type oligosaccharide enhances the antibody-dependent cellular cytotoxicity of single-gene-encoded bispecific antibody comprising of two single-chain antibodies linked to the antibody constant region. J Biochem. 2006;140:359–68.
10. Boyle JS, Silva A, Brady JL, Lew AM. DNA immunization: induction of higher avidity antibody and effect of route on T cell cytotoxicity. Proc Natl Acad Sci U S A. 1997;94:14626–31.
11. Greenspan JS, Gadol N, Olson JA, Talal N. Antibody-dependent cellular cytotoxicity in recurrent aphthous ulceration. Clin Exp Immunol. 1981;44:603–10.
12. Chang MI, Panorchan P, Dobrowsky TM, Tseng Y, Wirtz D. Single-molecule analysis of human immunodeficiency virus type 1 gp120-receptor interactions in living cells. J Virol. 2005;79:14748–55.
13. Kanai S, Liu J, Patapoff TW, Shire SJ. Reversible self-association of a concentrated monoclonal antibody solution mediated by Fab-Fab interaction that impacts solution viscosity. J Pharm Sci. 2008;10:4219–27.
14. Liu J, Nguyen MD, Andya JD, Shire SJ. Reversible self-association increases the viscosity of a concentrated monoclonal antibody in aqueous solution. J Pharm Sci. 2005;94:1928–40.
15. Moore JM, Patapoff TW, Cromwell ME. Kinetics and thermodynamics of dimer formation and dissociation for a recombinant humanized monoclonal antibody to vascular endothelial growth factor. Biochemistry. 1999;38:13960–7.
16. Vialtel P, Kells DI, Pinteric L, Dorrington KJ, Klein M. Nucleation-controlled polymerization of human monoclonal immunoglobulin G cryoglobulins. J Biol Chem. 1982;257:3811–8.
17. Gupta RC, Laforce FM, Mills DM. Polymorphonuclear leukocyte inclusions and impaired bacterial killing in patients with Felty's syndrome. J Lab Clin Med. 1976;88:183–93.
18. Stoebner P, Renversez JC, Groulade J, Vialtel P, Cordonnier D. Ultrastructural study of human IgG and IgG-IgM crystalcryoglobulins. Am J Clin Pathol. 1979;71:404–10.
19. Podell DN, Packman CH, Maniloff J, Abraham GN. Characterization of monoclonal IgG cryoglobulins: fine-structural and morphological analysis. Blood. 1987;69:677–81.
20. Minton AP. Macromolecular crowding. Curr Biol. 2006;16:R269–71.
21. Perham M, Stagg L, Wittung-Stafshede P. Macromolecular crowding increases structural content of folded proteins. FEBS Lett. 2007;581:5065–9.
22. Zhang F, Skoda MW, Jacobs RM, Martin RA, Martin CM, Schreiber F. Protein interactions studied by SAXS: effect of ionic strength and protein concentration for BSA in aqueous solutions. J Phys Chem B. 2007;111:251–9.
23. Liu Y, Fratini E, Baglioni P, Chen WR, Chen SH. Effective long-range attraction between protein molecules in solutions studied by small angle neutron scattering. Phys Rev Lett. 2005;95:118102.
24. Poskittand TR, Poskitt PK. Temperature dependent activation of the alternate complement pathway by an IgG cryoglobulin. Am J Hematol. 1979;7:147–54.

25. Cromwell ME, Hilario E, Jacobson F. Protein aggregation and bioprocessing. AAPS J. 2006;8:E572–9.
26. Yang MX, Shenoy B, Disttler M, Patel R, McGrath M, Pechenov S, *et al*. Crystalline monoclonal antibodies for subcutaneous delivery. Proc Natl Acad Sci U S A. 2003;100:6934–9.
27. Qi M, Steiger G, Schifferli JA. A calcium-dependent cryoglobulin IgM kappa/polyclonal IgG. J Immunol. 1992;149:2345–51.
28. Durant JA, Chen C, Laue TM, Moody TP, Allison SA. Use of T4 lysozyme charge mutants to examine electrophoretic models. Biophys Chem. 2002;101–102:593–609.
29. Moody TP, Kingsbury JS, Durant JA, Wilson TJ, Chase SF, Laue TM. Valence and anion binding of bovine ribonuclease A between pH 6 and 8. Anal Biochem. 2005;336:243–52.
30. Esue O, Cordero M, Wirtz D, Tseng Y. The assembly of MreB, a prokaryotic homolog of actin. J Biol Chem. 2005;280:2628–35.
31. Carlier MF. Control of actin dynamics. Curr Opin Cell Biol. 1998;10:45–51.
32. Kovar DR, Harris ES, Mahaffy R, Higgs HN, Pollard TD. Control of the assembly of ATP- and ADP-actin by formins and profilin. Cell. 2006;124:423–35.
33. Coulombe PA, Bousquet O, Ma L, Yamada S, Wirtz D. The 'ins' and 'outs' of intermediate filament organization. Trends Cell Biol. 2000;10:420–8.
34. Heidemannand SR, Wirtz D. Towards a regional approach to cell mechanics. Trends Cell Biol. 2004;14:160–6.
35. Liu YC, Yang ZY, Du J, Yao XJ, Lei RX, Zheng XD, *et al*. Study on the interactions of kaempferol and quercetin with intravenous immunoglobulin by fluorescence quenching, fourier transformation infrared spectroscopy and circular dichroism spectroscopy. Chem Pharm Bull (Tokyo). 2008;56:443–51.
36. Rahmelowand K, Hubner W. Secondary structure determination of proteins in aqueous solution by infrared spectroscopy: a comparison of multivariate data analysis methods. Anal Biochem. 1996;241:5–13.
37. Tseng Y, An KM, Wirtz D. Microheterogeneity controls the rate of gelation of actin filament networks. J Biol Chem. 2002;277:18143–50.
38. Panzerand S, Thaler E. An acquired cryoglobulinemia which inhibits fibrin polymerization in a patient with IgG kappa myeloma. Haemostasis. 1993;23:69–76.
39. Esue O, Carson AA, Tseng Y, Wirtz D. A direct interaction between actin and vimentin filaments mediated by the tail domain of vimentin. J Biol Chem. 2006;281:30393–9.
40. Janssen KP, Eichinger L, Janmey PA, Noegel AA, Schliwa M, Witke W, *et al*. Viscoelastic properties of F-actin solutions in the presence of normal and mutated actin-binding proteins. Arch Biochem Biophys. 1996;325:183–9.
41. Liu Y, Chen SH, Berti D, Baglioni P, Alatas A, Sinn H, *et al*. Effects of counterion valency on the damping of phonons propagating along the axial direction of liquid-crystalline DNA. J Chem Phys. 2005;123:214909.
42. Javid N, Vogtt K, Krywka C, Tolan M, Winter R. Capturing the interaction potential of amyloidogenic proteins. Phys Rev Lett. 2007;99:028101.
43. Giacometti A, Gazzillo D, Pastore G, Das TK. Numerical study of a binary Yukawa model in regimes characteristic of globular proteins in solutions. Phys Rev E Stat Nonlin Soft Matter Phys. 2005;71:031108.
44. Jin L, Yu YX, Gao GH. A molecular-thermodynamic model for the interactions between globular proteins in aqueous solutions: applications to bovine serum albumin (BSA), lysozyme, alpha-chymotrypsin, and immuno-gamma-globulins (IgG) solutions. J Colloid Interface Sci. 2006;304:77–83.
45. Edwards S, Doi M. The theory of polymer dynamics. New York: Oxford University Press; 1986.
46. Higgins JS, Benoit HC. Polymers and neutron scattering. New York: Oxford University Press; 1994.
47. Tseng Y, Fedorov E, McCaffery JM, Almo SC, Wirtz D. Micromechanics and ultrastructure of actin filament networks crosslinked by human fascin: a comparison with alpha-actinin. J Mol Biol. 2001;310:351–66.
48. Tseng Y, An KM, Esue O, Wirtz D. The bimodal role of filamin in controlling the architecture and mechanics of F-actin networks. J Biol Chem. 2004;279:1819–26.